

Analysis of the Local Structure around Eu and Mn Ions in Alkaline-Earth Silicate Phosphors for White Light Illumination

Kaoru Okamoto^{*}, Masahiko Yoshino^{*}, Motoyuki Shigeiwa^{*}, Masayoshi Mikami^{*}, Toshio Akai^{*}, Naoto Kijima^{*}, Tetsuo Honma[†], and Masaharu Nomura[‡]

^{*} Mitsubishi Chemical Group Science and Technology Research Center, Inc., 1000 Kamoshida-cho, Aoba-ku, Yokohama, 227-8502 Japan

[†] Japan Synchrotron Radiation Research Institute, 1-1-1, Kouto, Sayo-cho, Sayo-gun, Hyogo, 679-5198 Japan

[‡] High Energy Accelerator Research Organization, 1-1 Oho, Tsukuba, Ibaraki, 305-0801 Japan

Abstract. M_2SiO_4 -based phosphors (M : alkaline-earth metal) that emit red to blue light are expected to offer high color rendering to white light-emitting diodes (LEDs) in combination with blue or near-UV excitation sources. It is very important for the complete control of the emission color to understand the crystal field around the active elements (rare-earth and transition metals). XAFS spectroscopy is applied to a $(Ba,Ca)_2SiO_4:Eu,Mn$ phosphor at Eu L₃- and Ba, Ca, Eu, Mn K-edges to elucidate the local environments of Eu and Mn. Eu L₃- and Mn K-edge XANES spectra showed that Eu and Mn are both divalent, like Ba and Ca. K-edge EXAFS spectra indicated that the local structures of Eu and Mn are similar to those of Ba and Ca, respectively. However, the curve-fitting analysis showed that the first coordination shell of Eu has two Eu–O bonds that are both shorter than the Ba–O bond. FEFF calculations were also performed based on a BaCaSiO₄ model constructed from the crystal structure of KNaSO₄. They suggested that Eu substitutes both of Ba and Ca sites with some structural modification while Mn is clearly at the octahedral Ca site that is the smallest of the substitution sites.

Keywords: phosphor, rare-earth metal, local structure, XAFS.

PACS: 61.10.Ht, 87.64.Fb, 78.55.-m

INTRODUCTION

White light emitting diodes (LED) are one of the promising illumination sources. Its strength is being compact, Hg-free, and energy-efficient, but the color rendering properties should be further improved. Light from the existing white LEDs looks somewhat pale, because white color is obtained by the combination of blue LEDs and yellow phosphors. The easiest and most reliable way to solve the problem is using red-green-blue (RGB) combinations of phosphors and excitation sources.

Doped alkaline-earth silicates with rare earth and/or transition metals work as phosphors by near-UV excitation [1,2]. They have an ideal characteristic for RGB-LEDs that the color changes from red to blue through green according to the concentration of dopants and the composition of alkaline-earth metals. Structural information around the active ions is very important to achieve the complete color control. In this study, we investigated the local structures of Eu

and Mn in a $(Ba,Ca)_2SiO_4:Eu,Mn$ (BCS:Eu,Mn) phosphor by XAFS spectroscopy to study how Eu and Mn exist in the host material.

EXPERIMENTAL

$Ba_{1.5}Ca_{0.5}SiO_4:Eu_{0.15}Mn_{0.05}$ was synthesized by solid-state reaction. A stoichiometric mixture of $BaCO_3$, $CaCO_3$, Eu_2O_3 , $MnCO_3$, and SiO_2 were calcined in the presence of NH_4Cl and C under $H_2(4\%)+N_2$ atmosphere at 1200°C for 6 hours. Ba, Ca, Eu, and Mn K-edge and Eu L₃-edge XAFS measurements were carried out at BL19B2 at SPring-8 (Japan Synchrotron Radiation Research Institute, Hyogo, Japan) and at BL-9A in Photon Factory (Institute of Materials Structure Science, High Energy Accelerator Research Organization, Tsukuba, Japan) [3]. Eu and Ba K-edge measurements were performed in transmission mode using a Si(311) double-crystal monochromator and ion chambers filled with Ar75%-Kr25% and Kr gases for I_0 and I , respectively. Eu L₃-

edge and Mn K-edge data were measured in the fluorescent X-ray yield mode using a Si(111) double-crystal monochromator, an I_0 chamber filled with N₂, and a 16-element Ge-SSD. Ca K-edge measurements were also in the fluorescent X-ray yield mode but using an I_0 chamber filled with He and a Lytle detector filled with Ar.

The obtained data were processed according to the conventional procedure [4]: pre-edge background subtraction using Victoreen-like functions and normalization for XANES, and subsequent atomic absorption subtraction using cubic-spline functions for EXAFS. EXAFS functions were used as $k^3\chi(k)$, where k is the wavenumber of electron. Data analysis was performed using EXAFSH [5] and FEFF8.20 [6] codes.

RESULTS AND DISCUSSION

Figures 1 and 2 show the Eu L₃-edge and Mn K-edge XANES spectra of BCS:Eu,Mn, together with those for reference compounds: BaMgAl₁₀O₁₇:Eu^{II} [7], Eu^{III}₂O₃, and Mn^{II}(CH₃COO)₂·4H₂O. The peak positions clearly exhibit that Eu and Mn ions are both divalent in BCS:Eu,Mn. It is also suggested that they substitute Ba²⁺ and Ca²⁺ ions in the host materials that have the same oxidation states.

Figure 3 shows the K-edge EXAFS spectra $k^3\chi(k)$ of Ba, Eu, Ca, and Mn in BCS:Eu,Mn. EXAFS of Eu and Mn are very similar to those of Ba and Ca, respectively, indicating similarity in their sites. However, the corresponding Fourier transforms in Fig. 4 imply that the local structures are not strictly the same. Each of them has two prominent peaks attributable to M–O and M–Ba, Ca, Si. While the latter peak is at around 3 Å in every case, the peak position of the former varies from 1.5 Å for Mn to 2.2 Å for Ba. The order of the peak position is the same as that of the ionic radius; Mn²⁺ (1.10 Å) < Ca²⁺ (1.26 Å) < Eu²⁺ (1.39 Å) < Ba²⁺ (1.56 Å), where values in parentheses are the ionic radii in 8-coordinated compounds [8].

EXAFS curve-fitting analysis was performed for Ba–O and Eu–O peaks in back-Fourier-transformed k space for the k and R ranges of 4–12 Å⁻¹ and 1.5–2.4 Å, respectively. Standard amplitudes and phase shifts were extracted from EXAFS functions calculated by FEFF8.20. Although detailed investigation of Eu–O shells failed due to the limited data ranges compared to the complexity of the local structure, the curve-fitting analysis suggested that the Eu–O peak contains two shells at around 2.2–2.3 Å and 2.5 Å, which are both shorter than a single Ba–O shell at 2.75 Å. These results show that Eu substitutes a slightly larger site

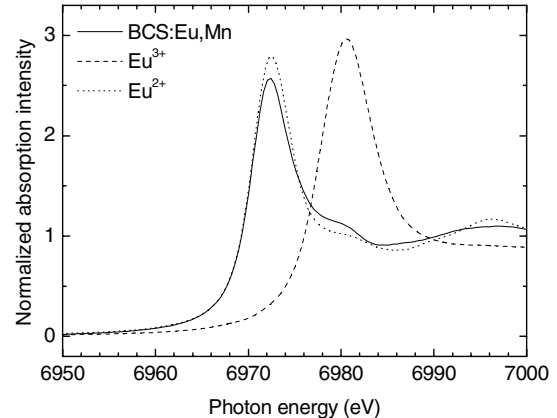


FIGURE 1. Eu L₃-edge XANES spectra.

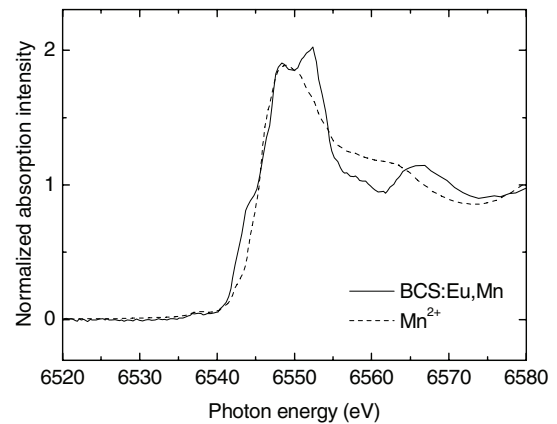


FIGURE 2. Mn K-edge XANES spectra.

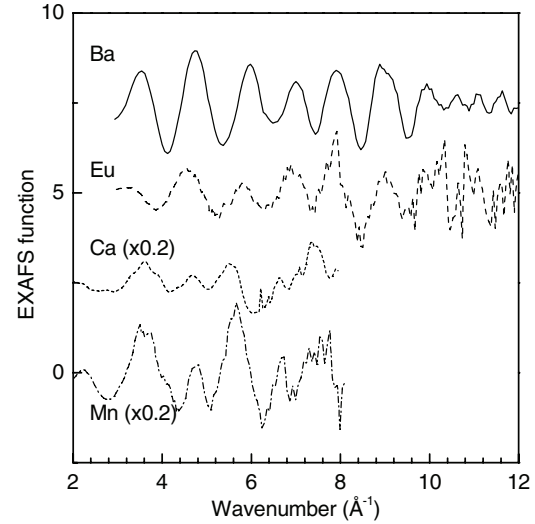


FIGURE 3. K-edge EXAFS spectra.

with some structural modification to reduce the potential energy.

To determine the substitution site, FEFF simulation was performed. The plausible crystal structure of Ba_{2-x}Ca_xSiO₄ (0.4 ≤ x < 1) is hexagonal (P3m1) [9,10], and KNaSO₄ [11] was selected as the structural model

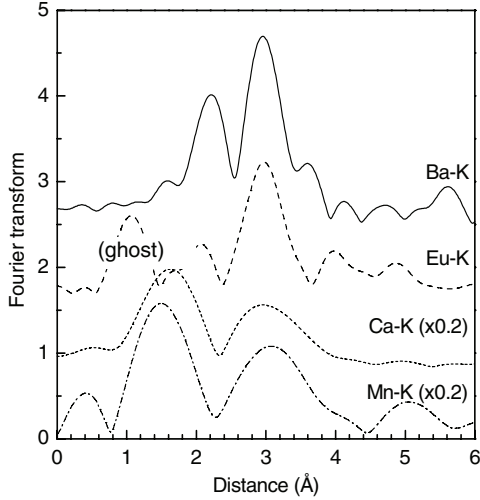


FIGURE 4. K-edge EXAFS Fourier transforms. The phase shifts are not corrected.

for FEFF calculations. K, Na, and S were substituted by Ba, Ca, and Si, respectively, and the crystal structure was optimized by the first-principles calculation code ABINIT [12]. FEFF calculation was applied for each of the three Ba and Ca sites in this structural model: an elongated trigonal antiprism site, Ba1, an octahedral site, Ca1, and a 10-coordinated site, Ba2/Ca2.

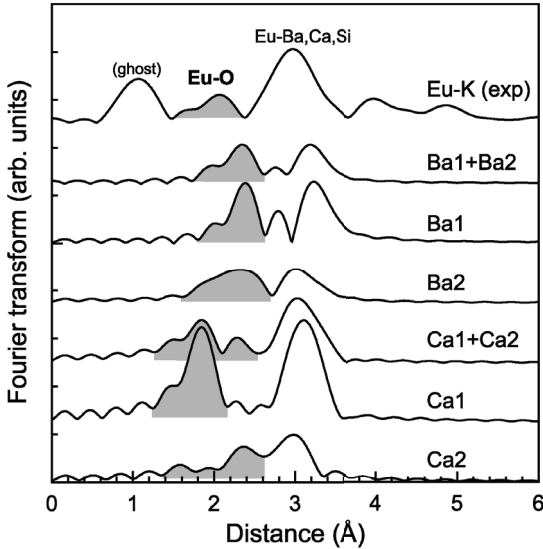


FIGURE 5. Experimental and simulated Eu K-edge EXAFS Fourier transforms. The gray areas indicate the Eu–O peaks.

Figure 5 compares the simulated Fourier transforms of Ba1/2, Ca1/2, and averaged Ba/Ca sites (Ba1+Ba2 and Ca1+Ca2) with the experimental data. It reveals that the experimental Fourier transform can be reproduced by neither those of a particular sites nor

the averages. The multi-peak nature of Eu–O at the Ba2/Ca2 site implies that Eu could substitute the Ba2/Ca2 site with some structural modification. Meanwhile, Ca1 is the only site that gives a short Eu–O distance as 2.2–2.3 Å, although it seems too small for Eu²⁺. It can be concluded that these two sites, Ba2/Ca2 and Ca1, may be the candidates for the Eu site. On the other hand, the FEFF result for Mn (Fig. 6) obviously shows that Mn substitutes the Ca1 site. Ca1 is the smallest site among the three sites and only small contraction is required on Mn²⁺ substitution.

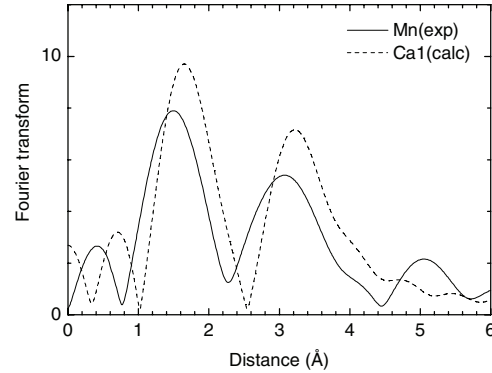


FIGURE 6. Experimental and simulated Mn K-edge EXAFS Fourier transforms.

REFERENCES

1. J. K. Park, M. A. Lim, C. H. Kim, H. D. Park, J. T. Park, and S. Y. Choi, *Appl. Phys. Lett.* **82**, 683–685 (2003).
2. J. S. Kim, Y. H. Park, J. C. Choi, and H. L. Park, *J. Electrochem. Soc.* **152**, H135–H137 (2005).
3. M. Nomura and A. Koyama, *J. Synchrotron Rad.* **6**, 182–184 (1999).
4. For a review, D. C. Koningsberger and R. Prince, Editors, *X-ray Absorption: Principle, Applications, Techniques of EXAFS, SEXAFS and XANES*, New York: Wiley Interscience, 1988.
5. T. Yokoyama, H. Hamamatsu, and T. Ohta, Computer code EXAFSH, Version 2.1, the University of Tokyo, 1993.
6. A. L. Ankudinov, B. Ravel, J. J. Rehr, and S. D. Conradson, *Phys. Rev. B*, **58**, 7565–7576 (1998).
7. I. Hirosawa, T. Honma, K. Kato, N. Kijima, and Y. Shimomura, *J. Soc. Inf. Display* **12**, 269–273 (2004).
8. R. D. Shannon, *Acta Cryst.* **A32**, 751–767 (1976).
9. J. G. Thompson, R. L. Withers, and B. G. Hyde, *J. Am. Ceram. Soc.* **70**, C383–C386 (1987).
10. C. Brisi, *Ind. Ital. Cem.* **33**, 397–402 (1963).
11. K. Okada and J. Ossaka, *Acta. Cryst.* **B36**, 919–921 (1980).
12. X. Gonze, J.-M. Beuken, R. Caracas, F. Detraux, M. Fuchs, G.-M. Rignanese, L. Sindic, M. Verstraete, G. Zerah, F. Jollet, M. Torrent, A. Roy, M. Mikami, Ph. Ghosez, J.-Y. Raty, and D.C. Allan, *Comput. Mater. Sci.* **25**, 478–492 (2002); <http://www.abinit.org>.